FEBS Letters 587 (2013) 2164–2172

FEBS Letters

journal homepage: www.FEBSLetters.org

Reactive oxygen species promote chloroplast dysfunction and salicylic acid accumulation in fumonisin B1-induced cell death

Fuqiang Xing, Zhe Li, Aizhen Sun, Da Xing *

MOE Key Laboratory of Laser Life Science & Institute of Laser Life Science, College of Biophotonics, South China Normal University, Guangzhou 510631, China

ARTICLE INFO

Article history:
Received 13 March 2013
Revised 19 April 2013
Accepted 5 May 2013
Available online 24 May 2013

Edited by Miguel De la Rosa

Keywords:
Chloroplast dysfunction
Fumonisin B1
Programmed cell death
Phenylalanine ammonia lyase
Reactive oxygen species
Salicylic acid

ABSTRACT

We report a novel regulatory mechanism by which reactive oxygen species (ROS) regulate fumonisin B1 (FB1)-induced cell death. We found that FB1 induction of light-dependent ROS production promoted the degradation of GFP-labeled chloroplast proteins and increased phenylalanine ammonia lyase (PAL) activity, *PAL1* gene expression and SA content, while pretreatment with ROS manipulators reversed these trends. Moreover, treatment with H_2O_2 or 3-amino-1,2,4-triazole increased PAL activity, *PAL1* gene expression and SA content. PAL inhibitor significantly blocked FB1-induced lesion formation and SA increase. Our results demonstrate that light-dependent ROS accumulation stimulates the degradation of chloroplastic proteins and up-regulates PAL-mediated SA synthesis, thus promoting FB1-induced light-dependent cell death.

1. Introduction

Plants have developed a complex immune system to resist pathogen attack. Hypersensitive response (HR) is a form of programmed cell death (PCD) as it leads to rapid, localized cell death at infection sites triggered by pathogens. Elicitor-induced hypersensitive cell death is a pathogen strategy for infection, whereas localized cell death at the site of infection is a plant defense strategy against pathogen attack [1,2]. Moreover, HR produced during some pathogen infection in plants has been recognized requiring the light [3,4]. However, further studies are needed to illustrate the underlying molecular mechanism of light-dependent HR cell death.

It is known that reactive oxygen species (ROS), in particular hydrogen peroxide (H_2O_2) and superoxide anion ($O_2^{\cdot -}$), are versatile molecules mediating a variety of cellular responses in both the animal and plant kingdoms. In animals, mitochondria have been recognized playing vital roles in ROS-dependent apoptotic cell death [5]. For instance, ROS act upstream of mitochondrial membrane depolarization, Bax relocalization, cytochrome *c* release, executing caspase activation and nuclear fragmentation [6,7]. In plants, besides mitochondria, chloroplasts are also important ROS suppliers, and they may generate intermediate signals involved in PCD. For example, the role of chloroplastic polyunsaturated fatty acids and phytochrome signaling during HR process suggest the participation of chloroplastic factor in the pathway leading to the HR cell death [4,8]. Our early studies showed that protoplasts exhibited an increase of ROS levels in a light-dependent manner after UV-C irradiation [9]. Recently, some studies demonstrated that various stimuli, such as aluminum toxicity, methyl jasmonate treatment and pathogen attack, can cause chloroplast dysfunction and photosynthetic damage as well as chloroplastic ROS production [10–12]. Studies showing the function of ROS in signal transduction networks during plant PCD process have started to emerge [13–15]. Although ROS generated in various cellular compartments of plants exposed to pathogens or elicitors are essential for the progress of HR. There are many functional roles of ROS, especially the signaling pathway leading to plant HR, remain largely unclear. For instance, it is not clear whether they interact with hormone signaling in triggering HR. Also, the direct role of ROS produced in different plant compartments needs to be illustrated.

Previous studies have utilized fumonisin B1 (FB1), a programmed cell death–eliciting mycotoxin produced by the *Fusarium moniliforme*, as a model system to investigate the role of cell death in plant–microbe interactions [16–18]. However, the exact

* Corresponding author. Fax: +86 20 85216052.
E-mail address: xingda@scnu.edu.cn (D. Xing).

0014-5793/$36.00
http://dx.doi.org/10.1016/j.febslet.2013.05.034

mechanism by which FB1 regulates light-dependent plant PCD is still largely unknown. Salicylic acid (SA) is a hormone signaling molecule functioning in plant-microbe interactions in the induction of HR. In addition, SA synthesis is influenced by the light condition and closely associated with the chloroplasts [19], indicating that chloroplasts play an important role in SA-mediated, light-dependent HR. Biochemical studies using isotope feeding demonstrate that a number of plants could synthesize SA from cinnamate, synthesized by phenylalanine ammonia lyase (PAL) from phenylalanine. However, whether SA is influenced by the early accumulation of ROS during the formation of HR and how ROS exert its regulating function are still unclear.

This study focuses on the investigation of the roles of ROS signals derived from chloroplasts on the oxidative damage to chloroplast morphology and function, as well as SA hormone signaling defenses in Arabidopsis (*Arabidopsis thaliana*) in order to reveal a novel molecular mechanism of fumonisin B1 (FB1)-triggered light-dependent cell death.

2. Materials and methods

2.1. Plant material and treatments

Plants of wild-type, transgenic Arabidopsis expressing stroma-targeted fluorescent protein (GFP) were all in the ecotype Columbia (Col-0) background. Plants were grown in soil culture with 16/8 h light/dark cycle (120 μmol quanta m^{-2} s^{-1}) and 82% relative humidity at 22 ± 1 °C. 4 weeks old plants were used for experiment. Stock solution of FB1 (7 mM) was prepared in methanol, and a final concentration of 10 μM (diluted in water) was used for treatments, with an equivalent volume of 0.14% methanol as controls.

For FB1 treatment, WT leaves were infiltrated with 10 μM FB1 or 0.14% methanol (control) using a 1 ml syringe without a needle and maintained in the presence or absence of light for indicated times. To manipulate ROS levels, we first treated plant leaves with ROS manipulators for 2 h by spraying 100 U ml^{-1} catalase (CAT), 1 mM ascorbic acid (AsA) or 10 μM 3-(3,4-dichlorophenyl)-1,1-dimethylurea (DCMU), then infiltrated with 10 μM FB1 for 4 d under the same growth conditions as described above.

For H_2O_2 treatment, the plants were excised the base of the stem and maintained in distilled water for 1 h to eliminate wound stress, then the cut ends of the stems were kept in a small growth chamber wrapped with aluminium foil containing 5 mM H_2O_2 for 1–4 days at 22 ± 1 °C. For 3-amino-1,2,4-triazole (3-AT) treatment, plant leaves were sprayed with 15 mM 3-AT for 1–4 days, then the leave samples were collected and immediately frozen with liquid nitrogen for further analysis.

2.2. Histochemical staining

In situ detection of $O_2^{\cdot-}$ and H_2O_2 accumulation was performed using nitro blue tetrazolium (NBT) and 3,3′-diaminobenzidine (DAB) histochemical staining [11], respectively. Leaves after different treatment were detached from plants and submerged in NBT solution (1 mg ml^{-1} NBT plus 10 mM NaN_3 solution in 10 mM potassium phosphate buffer pH 7.8) or DAB solution (1 mg ml^{-1}, pH 5.5). After leaves stained for 40 min (NBT) or 2 h (DAB), then leaves were boiled in 95% ethanol for 15 min to remove the chlorophyll completely and stored in 60% glycerol for observation and photos taking.

To observe the dying cells in FB1-induced Arabidopsis leaves, Evans blue staining was performed as described [20]. Detached leaves were submerged in Evans blue solution (0.25%, w/v) for 5 h. Then the leaves were boiled in 95% ethanol for 15 min to remove the chlorophyll completely for observation and photos taking. The blue precipitates were solubilized with 1% (w/v) SDS in 50% (v/v) methanol at 50 °C for 20 min and quantified by measuring the absorbance at 600 nm.

2.3. GFP fluorescence analysis and chlorophyll quantification

Freshly prepared abaxial leaf strips expressing stroma-targeted GFP were incubated with treatments (10 μM FB1, 10 μM FB1 + 100 U ml^{-1} CAT, 10 μM FB1 + 1 mM AsA) or 0.14% methanol (Control) in 10 mM MES–NaOH (pH 5.5) at 23 °C for 5–48 h. The leaf strips were then placed in a small Petri dish containing 10 mM MES–NaOH (pH 5.5). Then microscopic observations were performed using a Zeiss LSM 510 META laser confocal scanning microscope (Zeiss, Jena, Germany). The GFP signal was visualized with excitation at 488 nm and emission at 500–550 nm using a band pass filter, and chlorophyll fluorescence (488 nm excitation) was visualized at 650 nm with a long pass filter. Various treated leaf strips were placed flat onto a plastic holder and fixed at both ends with silicon grease and the GFP fluorescence signal was measured in a luminescence spectrometer (Perkin–Elmer, LS55, UK), with an excitation wavelength of 488 nm and emission wavelengths between 500 and 600 nm (a slit width of 2.5 nm). The fluorescence intensity at 525 nm was used to quantify the relative GFP fluorescence.

The chlorophyll contents were measured according to Arnon [21]. Samples were ground in 95% ethanol together with 150 mg of washed quartz sand under dim light and homogenized for 5 min at 4 °C. The concentration was determined by spectrophotometric analysis of extracts of leaves in 95% ethanol at 649 and 665 nm.

2.4. Total RNA isolation and quantitative reverse transcript-PCR (qRT-PCR)

Total RNA was extracted according to the manufacturer's specifications using the TRIZOL reagent (Invitrogen). First-strand cDNA was synthesized with the SuperScript II First-Strand Synthesis System (Invitrogen) and cDNA were used as a template in PCR reactions with gene-specific primers (designed and synthesized by Sangon Biotech, Shanghai). Quantitative real time PCR (qRT-PCR) was performed using the Roche lightCycler™ 2.0 Real-time PCR Detection System. The relative abundance of *Actin2* was determined and used as the internal standard. PCR was performed using the following primers.

Actin2: (5′-AACGATTCCTGGACCTGCCTCATCATACTC-3′ and 5′-AGAGATTCAGATGCCCAGAAGTCTTGTTCC-3′).

PAL1 (5′-AACGGAGGAGGAGTGGACG-3′ and 5′-CTTTCATTTGCTC CGCTGC-3′).

2.5. PAL activity assay

PAL activity was determined according to a previous reported method with minor modifications [22]. Crude protein was extracted from samples stored at −78 °C. A 0.1 g sample was ground into a fine powder with liquid nitrogen and homogenized for 5 min at 4 °C in 1 ml of 0.1 M borate buffer (pH 8.8) containing 5% polyvinylpyrrolidone, 20 mM β-mercaptoethanol, and 1 mM EDTA. The mixture was centrifuged at 13400 rpm at 4 °C for 10 min. The supernatant was defined as a crude protein extract. Reaction mixtures consisting of 3.9 mL 0.1 M borate buffer (pH 8.8) and 100 μl enzyme extracts were preincubated at 37 °C (5 min) and the reaction was started by adding 1 mL 50 mM L-phenylalanine (Sigma–Aldrich, China). The mixture was incubated at 37 °C for 2 h and stopped by adding 0.2 mL 6 M HCl. PAL activity was assayed by measuring absorbance at 290 nm because of the release of

trans-cinnamate. Controls contained only enzyme solution and buffer. Increase in $OD_{290\ nm}$ was recorded using an LS 55 Luminescence Spectrophotometer (PerkinElmer, LS55, UK) to calculate the production of *trans*-cinnamate. Protein concentration was assayed with bovine serum albumin as the standard by the method of Bradford.

2.6. Quantitation of SA

The extraction and total SA (free SA and SA conjugate) was performed according to a previous method [23]. Briefly, plant tissues were stored in liquid nitrogen after the different treatments. For each sample, ~0.5 g of the frozen tissue was ground in 1 mL of 90% methanol and centrifuged at ~10000*g* for 15 min. The pellet was back extracted with 0.5 mL of 100% methanol and centrifuged. Methanol extracts were combined, and dried at 40 °C under vacuum. The residue was resuspended in either 2.5 mL of 5% trichloroacetic acid and sonicated for 10 min. Free SA was extracted into 2 volumes of cyclopentane/ethyl acetate (1:1). The organic extract was dried under nitrogen and analyzed by HPLC. The amount of SA conjugate was indirectly quantified by acid hydrolyzing the compounds that remained in the aqueous phase. The aqueous phase was acidified with HCl to pH 1 and boiled at 80 °C for 60 min. Then extracting free SA with the organic mixture was performed and analyzed as above.

3. Results

3.1. Light-dependent ROS production is associated with FB1-induced cell death

To test whether FB1 could induce light-dependent PCD phenotypes, Arabidopsis leaves were treated with 10 μM FB1 for 1–6 days. Consistent with our speculation, after the addition of FB1 in Arabidopsis leaves, macroscopic necrotic lesions formed only in the presence of light (Fig. 1A). As revealed by quantitative analysis in Fig. 1B, after FB1 treatment, the lesion on infiltrated leaves grown in the presence of light showed significant increase at 3 days and was obviously boosted at 4 days compared with those grown in the absence of light, suggesting that FB1-induced macroscopic lesion formed on the Arabidopsis leaves is light-dependent.

To determine whether FB1-induced ROS generation is light-dependent in leaves of Arabidopsis, we detached leaves after various treatments at 3 days and then stained in DAB and NBT solution. Our results showed that large stained area could be observed if the leaves infected with FB1 for 3 days in the presence of light (Fig. 1C). Microscopic analysis revealed that DAB precipitates and NBT staining were mostly present in the chloroplasts (Fig. 1D). Moreover, histochemical assays of the ROS accumulation were consistent with the data obtained using confocal scanning microscope (Supplementary Figs. S2 and S3). In summary, these results suggest that

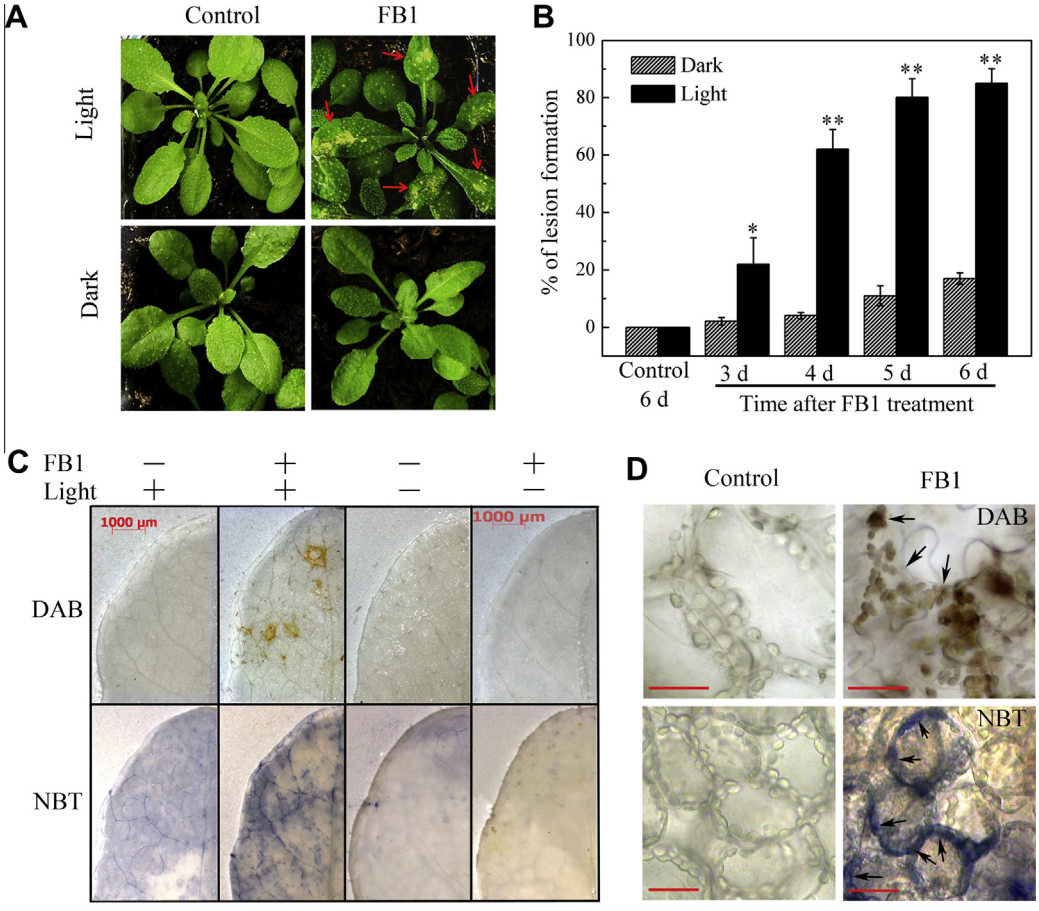

Fig. 1. Light-dependent ROS production is associated with FB1-induced HR-like cell death. (A) Lesion formation elicited by FB1. The leaves of 4-week-old Arabidopsis plants were infiltrated with or without 10 μM FB1 and grown in the presence (+) or absence (−) of light. Photographs were taken 4 days after different treatment in the plant leaves. Arrows show leaves with lesion formation. (B) Quantitative analysis of lesion formation on FB1-treated Arabidopsis leaves. Percentage of lesion formation is the lesion area per total area of leaves. Data are the mean ± S.D. ($n = 6$; $^{*}P < 0.05$ or $^{**}P < 0.01$ vs. control group). (C) The light-dependent ROS production in FB1-treated Arabidopsis leaves. Arabidopsis leaves were detached after various treatments at 3 days and then stained with 3,3-diaminobenzidine (DAB) or nitroblue tetrazolium (NBT) solution. The samples shown are representative of at least three independent experiments. Scale bars, 1000 μm. (D) Subcellular analysis of H_2O_2 and $O_2^{\cdot-}$ production using DAB and NBT staining at 3 days. Arrows show chloroplasts with DAB and NBT staining, respectively. FB1 10 μM, Control 0.14% methanol. Scale bars = 50 μm.

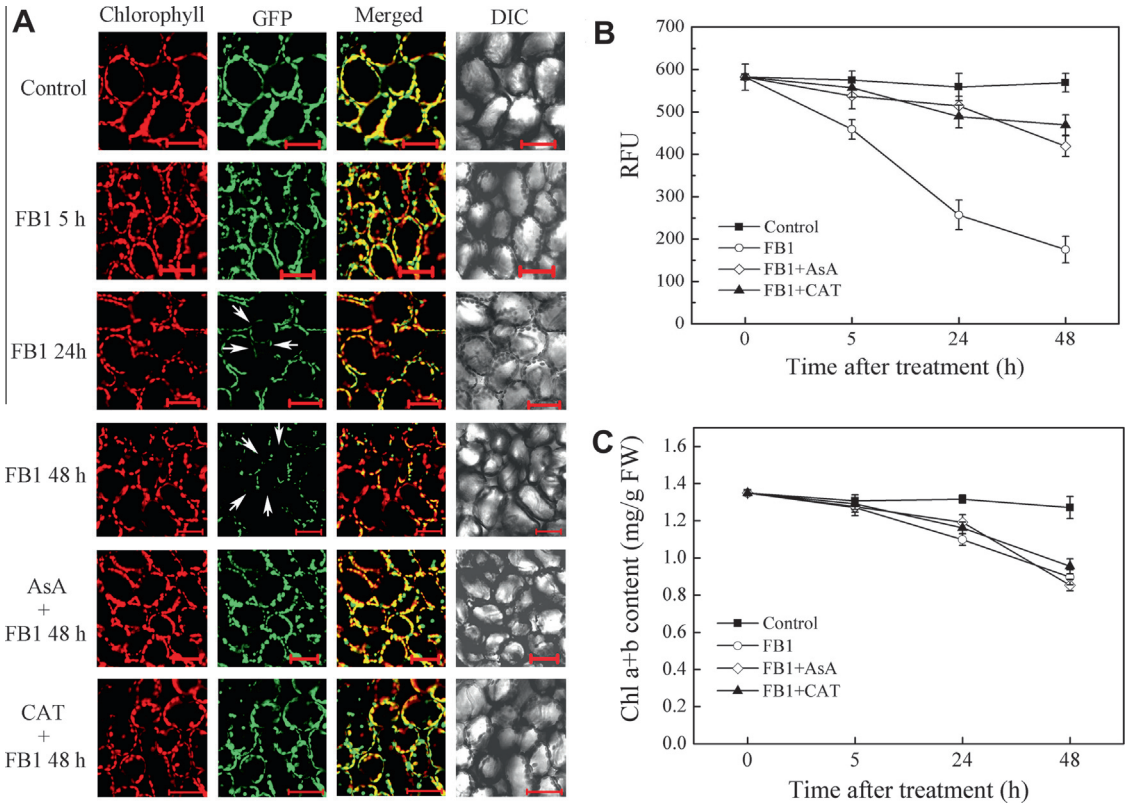

Fig. 2. FB1-induced chloroplast dysfunction is ROS dependent. (A) Photographs of the loss of stroma-targeted GFP fluorescence in Arabidopsis mesophyll cells. Fresh Arabidopsis leaves expressing stroma-targeted GFP were incubated with treatments (10 μM FB1, 10 μM FB1 + 100 U ml^{-1} CAT, 10 μM FB1 + 1 mM AsA) or 0.14% methanol (Control) in 10 mM MES–NaOH (pH 5.5) at 23 °C for 5–48 h and then observed by LSCM. GFP appears green, and chlorophyll fluorescence appears red. In merged images, the overlap of GFP and chlorophyll fluorescence appears yellow. The arrows indicate the location of the degradation of GFP-labeled protein in plant cells. Scale bars = 50 μm. (B) Time-dependent loss of GFP fluorescence in relative fluorescence units (RFU) after various treatments at different times in Arabidopsis leaves. (C) Changes in chlorophyll content after various treatments at different times in Arabidopsis leaves. FW, fresh weight. Each value was the means ± S.D. of three independent experiments.

FB1-induced ROS production is light-dependent and mainly derived from chloroplasts.

3.2. FB1-induced chloroplast protein degradation is ROS dependent

With the assistance of laser confocal scanning microscopy (LCSM), we examined FB1 application on the chloroplast integrity by monitoring the fluorescence distribution of the GFP in leaves of transgenic Arabidopsis that express a stroma-targeted GFP. Following incubation with treatments (10 μM FB1, 10 μM FB1 + 100 U ml^{-1} CAT, 10 μM FB1 + 1 mM AsA) or 0.14% methanol (Control) in 10 mM MES–NaOH (pH 5.5) at 23 °C for 0, 5, 24, 48 h, the microscopic observations were performed and the GFP fluorescence intensity was measured. As shown in Fig. 2A, under control conditions, no distribution of the fusion protein was seen in transgenic stroma-targeted GFP plants treated under continuous light. However, after treating these plants with 10 μM FB1 for 5 h, chloroplast integrity was impaired and the fusion protein was released from the chloroplast to the surrounding cytoplasm. During the next few hours, the intensities of GFP and chlorophyll fluorescence rapidly declined and loss of stromules was significant by 48 h under FB1 treatment in excised leaves, but this was significantly suppressed by incubation the abaxial leaf strips with AsA, a natural antioxidant; and CAT, a H_2O_2-specific scavenger, respectively (Fig. 2B). Together, impaired chloroplast integrity and the release of protein from the chloroplasts underwent significant changes with FB1 treatment, implying the involvement of the chloroplast dysfunction in promoting FB1-induced cell death. Moreover, treatment with FB1 led to a slower decline of chlorophyll content, with only ~16% of chlorophyll breakdown by 24 h and ~30% by 48 h compared with untreated plants. Interestingly, incubation the abaxial leaf strips with AsA and CAT appears not to block the decline of FB1-induced chlorophyll content (Fig. 2C). Our data suggest that ROS cause FB1-induced chloroplast protein degradation but have little effect on this chlorophyll breakdown.

3.3. FB1-induced PAL activation and SA synthesis is light-dependent

In order to further clarify the effects of light on PAL activity and SA content, we first analyzed the *PAL1* gene expression in FB1-treated Arabidopsis leaves. Results of qRT-PCR revealed that FB1 could promote significant increase of *PAL1* gene expression only in the presence of light at 2 and 4 days, suggesting that light mainly contribute to high expression of *PAL1* gene under FB1 treatment (Fig. 3A). The PAL activity and SA concentration were also analyzed in FB1-treated Arabidopsis leaves grown in the presence or absence of light at 2 and 4 days. As shown in Fig. 3B, C, the PAL activity and SA concentration showed similar increase with the result of *PAL1* gene expression (Fig. 3A). Collectively, these data suggest that FB1-induced PAL activation and SA synthesis is light-dependent.

3.4. ROS up-regulate PAL activity and SA synthesis during FB1 treatment

As shown above, FB1-induced chloroplastic ROS production and SA synthesis is light-dependent. To further establish a link between ROS and SA signaling in FB1-induced cell death, we hypothesize that ROS, as initial signaling molecular, play an important role in

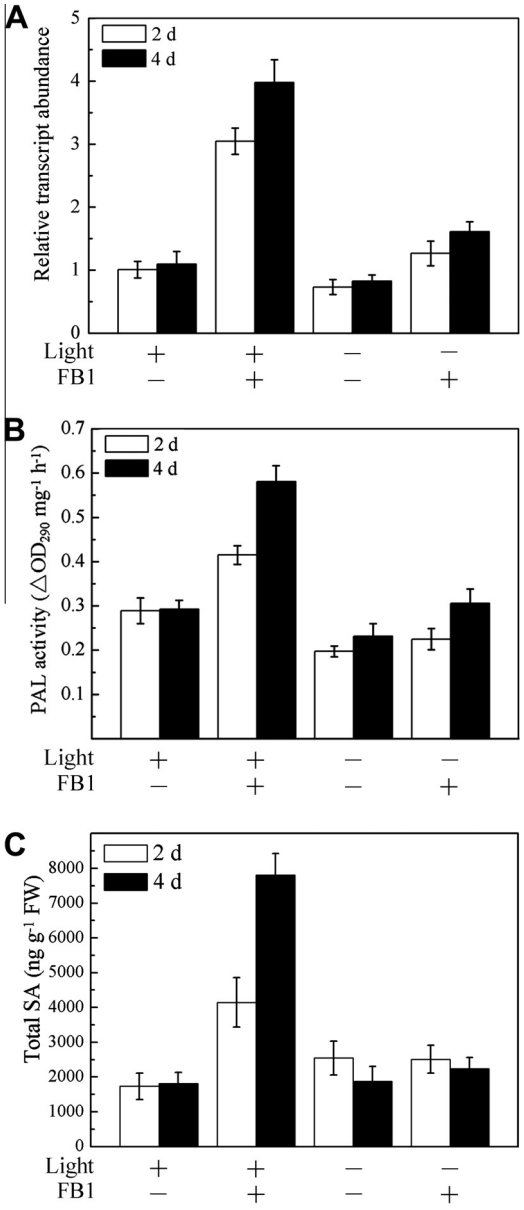

Fig. 3. FB1-induced PAL activation and SA synthesis is light-dependent. (A) Analysis of *PAL1* gene expression in differently treated plant leaves, using real-time PCR. The leaves of 4-week-old Arabidopsis plants were infiltrated with or without 10 μM FB1 and grown in the presence or absence of light for 2 or 4 days, then total RNA isolated and real-time PCR was performed. The *actin2* gene was used as an internal control (B) Determination of PAL activity in differently treated plant leaves at 2 or 4 days. PAL activity was determined from the yield of cinnamic acid, estimated by measuring A_{290} of the supernatant in extract. (C) Determination of total SA in differently treated plant leaves at 2 or 4 days. SA level was determined by HPLC methods. Data represent mean ± S.D. of three independent experiments.

the regulation of PAL activity and SA synthesis in FB1-induced cell death. In order to test this hypothesis, the effects of ROS manipulators (CAT, AsA, DCMU) on PAL activity, *PAL1* gene expression and SA content were assessed. DCMU (an inhibitor of photosynthetic electron transport) can be used to inhibit the ROS production in plant cells [14,24]. Experimental results showed that there was a high level of PAL mRNA and protein activity in comparison to mock-infiltrated controls, but pre-treatment with ROS manipulators significantly blocked these increase (Fig. 4A, C). This was companied by a similar change in SA level (Fig. 4E).

3.5. Exogenous H_2O_2 or 3-AT treatment enhances PAL activity and SA synthesis

To further confirm our hypothesis that ROS are involved in up-regulating PAL activity and SA synthesis, Arabidopsis leaves were treated with exogenous H_2O_2 or 3-AT. The intracellular ROS accumulation can be achieved by using 3-AT, a CAT inhibitor in plant [25]. In present study, experimental results showed that compared with water-treated controls, 3-AT and H_2O_2 treatment led to a time-dependent increase in PAL mRNA, protein activity, and SA level (Fig. 4B, D, F). Moreover, it was observed that in contrast with the increase of PAL activity, SA accumulation in H_2O_2-treated plant leaves was higher than in 3-AT-treated plant leaves within 1–4 days (Fig. 4D, F).

3.6. PAL inhibitor blocks FB1-induced SA synthesis and lesion formation

To investigate the roles of PAL in FB1-induced lesion formation, 4-week-old plants leaves were sprayed with 30 μM 2-aminoindane-2-phosphonic acid (AIP) for 2 h prior to FB1 treatment. AIP is a specific inhibitor of PAL enzyme [26]. In the present study, it was observed that visible lesion was formed on infiltrated leaves at 2 days after the addition of FB1, and was obviously increased at 4 days compared with the control group. As expected, pretreatment with AIP significantly blocked this increase (Fig. 5A, B), indicating that reducing PAL activity alleviated FB1-induced lesion formation on plant leaves. Using Evans Blue dye as a marker of cell death, the results obtained after infiltrating leaves with this dye and decolouring with methanol are shown in Fig. 5C. Plants treated with FB1 showed a higher capacity to fix the dye than the control plants, and the measurement of the Evans Blue extracted from leaves showed significant increase in plants treated with FB1 (Fig. 5D). However, pretreatment with AIP partially blocked the increase. These data suggest that PAL is required for FB1-induced lesion formation.

To further confirm that PAL is required for FB1-induced increase of SA synthesis, AIP was pre-incubated for 2 h in Arabidopsis leaves before the addition of FB1. We found that pretreatment with AIP strongly blocked the increase of PAL activity and SA content induced by FB1, suggesting that PAL is required for FB1-induced SA increase in Arabidopsis leaves (Fig. 5E, F).

4. Discussion

Although the contribution of ROS in the establishment of HR has been greatly appreciated, the possible mechanisms for ROS production and ROS-modulated signaling pathways in host plant cells are far from being completely understood. Several studies have shown that plant plasma membrane NADPH oxidases activity is required for pathogen-induced ROS production [27]. In addition to NADPH oxidases, class III plant peroxidases, oxalate oxidases and amine oxidases have also been proposed to generate ROS during pathogen attack in plants [28,29]. Additionally, Pastore et al. found that during oxidative stress, early generation of ROS can affect plant mitochondria by impairing metabolite transport, thus preventing further substrate oxidation, membrane potential generation and consequent large-scale ROS production [30]. Although most researches have focused on mitochondria as the generating source of ROS [1,31,32], recent studies have started to consider the necessity for the chloroplasts involvement in the pathway leading to the HR [33,34]. Indeed, chloroplasts as major ROS source in plant cells are largely based on over-reduction of the photosynthetic electron transport chain under excess excitation energy conditions, when the amount of energy exceeding that required for

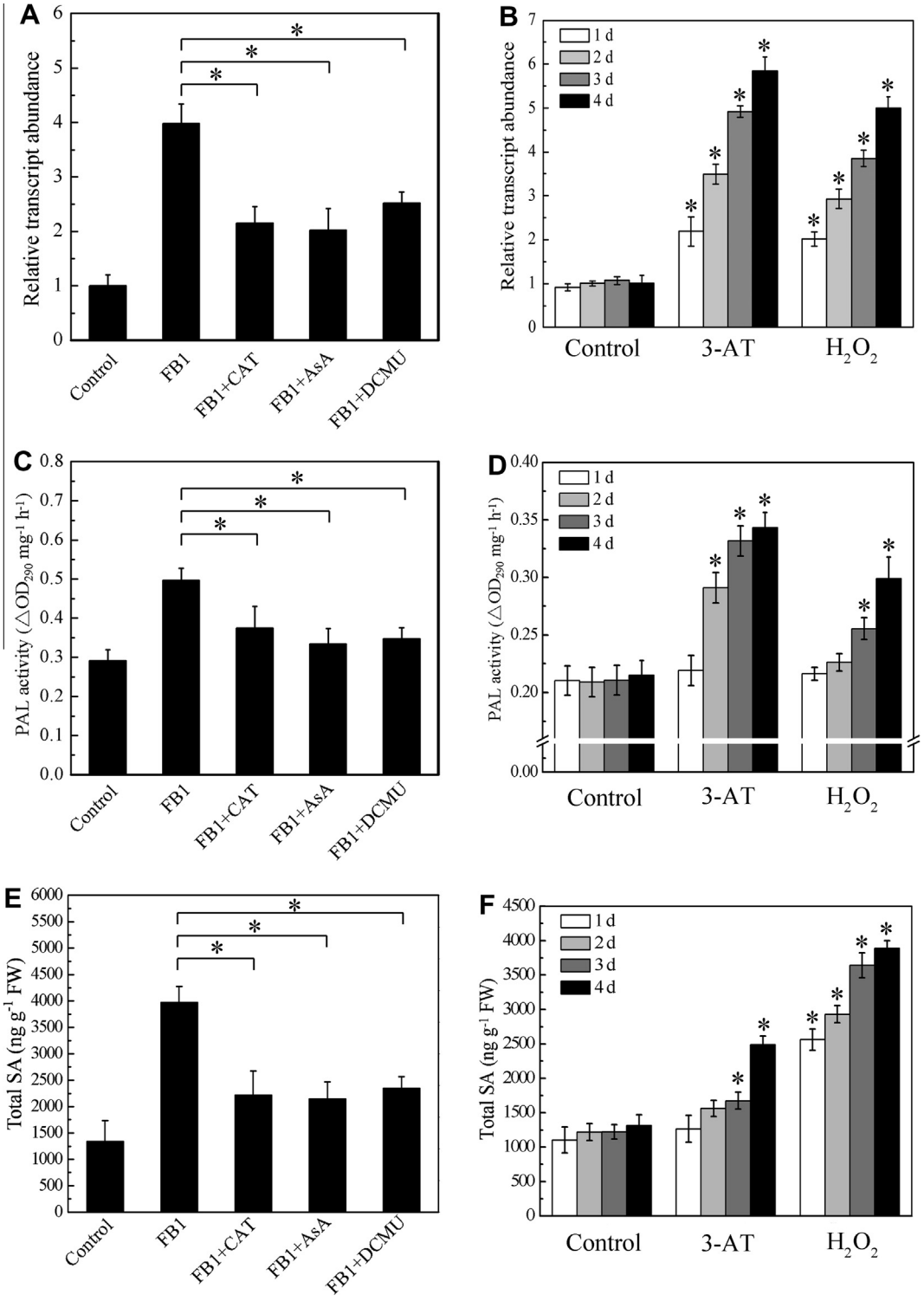

Fig. 4. ROS increase PAL activity, *PAL1* gene expression and SA content in leaves of Arabidopsis plants. (A, C, E) Effects of pretreatment with ROS manipulators on *PAL1* gene expression, PAL activity and SA level induced by FB1. Plant leaves were pre-treated with (100 U ml^{-1} CAT, 1 mM AsA, 10 μM DCMU) or without (Control) for 2 h and then infiltrated with 10 μM FB1 for 4 days. Data represent mean ± S.D. ($n = 3$; $^*P < 0.05$ vs. indicated group). (B, D, F) Effects of H_2O_2 and 3-AT treatment on *PAL1* gene expression, PAL activity and SA level. Plants leaves were treated with (5 mM H_2O_2, 15 mM 3-AT) or without (Control) for 1–4 d. The *actin2* gene was used as an internal control. Data represent mean ± S.D. ($n = 3$; $^*P < 0.05$ vs. control group).

photosynthetic CO_2 assimilation [35]. It has proposed that FB1-induced lesions on Arabidopsis leaves share some of the features of the HR lesions elicited by avirulent pathogens, including ROS accumulation at the margins of lesions [17]. However, whether ROS are produced in a light dependent manner and their subcellular production sites in plant cells remain to be determined. In the current study, our results showed that FB1 quickly induced light-dependent production of chloroplastic ROS including H_2O_2 and $O_2^{\cdot-}$ in plant leaves. (Figs. 1 and S2).

Several reports using GFP-labeled chloroplast proteins have shown that the degradation of chloroplast proteins in plants can occur under stress conditions (i.e., nutrient stress), and chloroplast

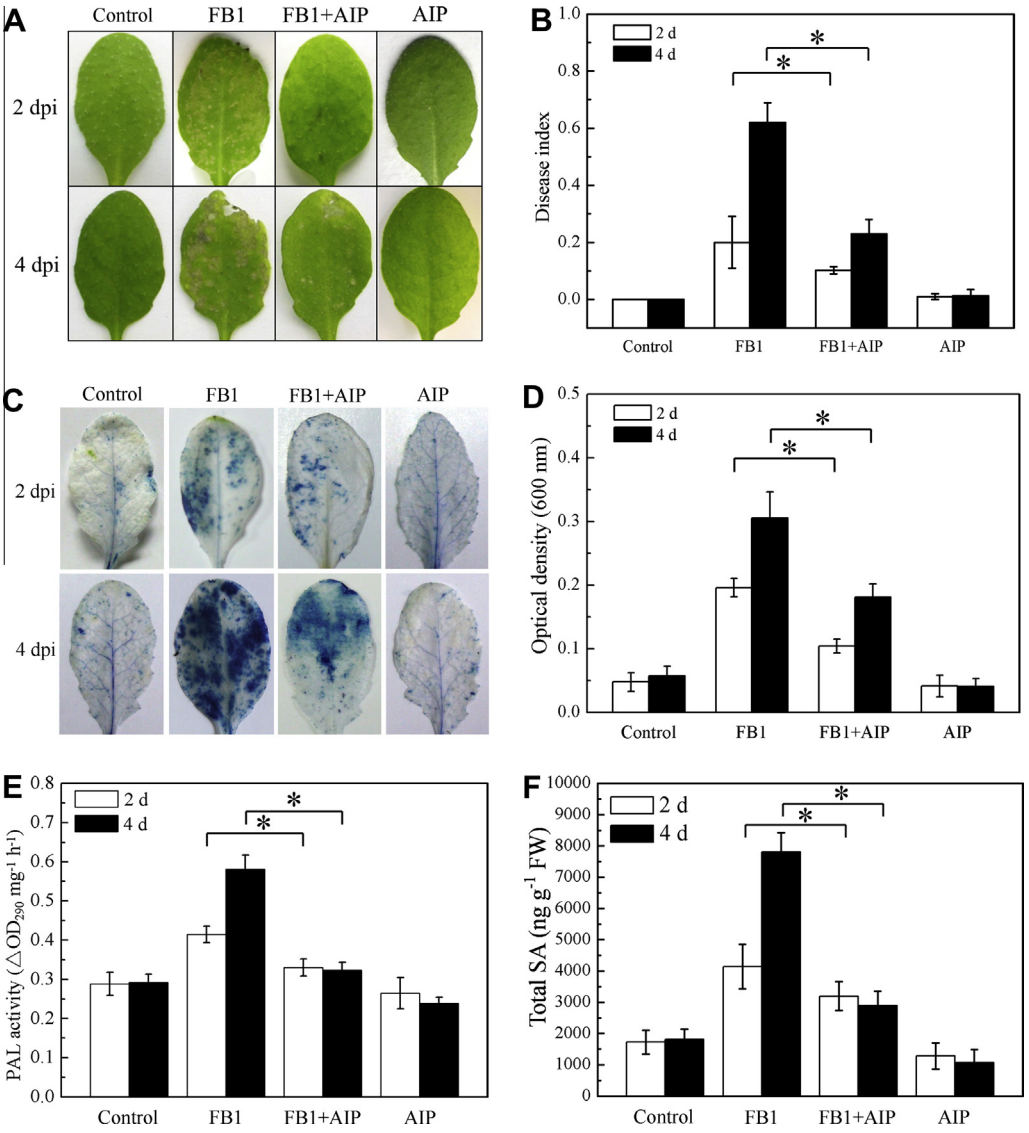

Fig. 5. Effects of PAL inhibitor (AIP) on FB1-induced lesion formation, PAL activity and SA level. (A) Phenotype of Arabidopsis leaves treated with 10 μM FB1 with or without pretreatment of 30 μM AIP. 4-week-old WT leaves were pre-treated or not with 30 μM AIP for 2 h, then infiltrated with 10 μM FB1 and grown in normal condition for 2 or 4 days. Photographs show representative leaves after different treatment. (B) Measurement of disease index after treated with 10 μM FB1 with or without pretreatment of 30 μM AIP. Disease index represent the mean of disease severities (0–1, light to severe). Data are the mean ± S.D. ($n = 6$; $^*P < 0.05$ vs. indicated group). (C) Evans Blue staining of leaves treated with 10 μM FB1 with or without pretreatment of 30 μM AIP. Cell death was assayed by Evans Blue staining in whole leaves after various treatments. (D) Quantitative analysis of the Evans Blue dye precipitates shown in (C), the precipitate was solubilized with 1% SDS in 50% (v/v) methanol at 50 °C and the optical density of solutions was measured at 600 nm. Data represent mean ± S.D. ($n = 3$; $^*P < 0.05$ vs. indicated group). (E, F) AIP suppressed the increase of PAL activity and SA content in FB-treated Arabidopsis leaves. Data represent mean ± S.D. ($n = 3$; $^*P < 0.05$ vs. indicated group).

proteins can be mobilized to the vacuole and then degraded by a variety of hydrolases [36,37]. However, whether FB1 treatment can also cause the degradation of chloroplast proteins and the molecular mechanism by which FB1 contributes to the degradation of chloroplast proteins under normal conditions have not been revealed. As photosynthetic organelles, chloroplast morphology is highly related to their energy and the cellular redox status, and may undergo some changes under many various stresses, which could provide some indication of their functional alteration. In order to further clarify the links between chloroplasts and the ROS-mediated immune system, we assessed the relative contribution and potential roles of ROS on the changes of chloroplast morphology using transgenic Arabidopsis expressing stroma-targeted GFP during FB1 stress. Experimental results show that chloroplastic ROS accumulation causes the degradation of chloroplast protein (Fig. 2). This provides the physiological evidence for the role of ROS in regulation of chloroplast-dependent immune response. Loss of chloroplast integrity preceding vacuole rupture and cellular collapse could be the initial steps triggering ROS-mediated HR. Identification of plant additional direct targets of ROS will be vital in addressing how specificity of ROS signaling is achieved during plant-pathogen interactions. Barna et al. found that the degradation of chlorophyll of damaged leaves is strongly induced by light [38]. In present study, FB1 treatment resulted in chlorophyll breakdown in the presence of light, but both AsA and CAT treatments had little effect on chlorophyll breakdown (Fig. 2C). These results suggest that FB1-induced chlorophyll breakdown is ROS independent and other mechanisms may be involved in this chlorophyll breakdown. Indeed, chloroplastic ROS are produced as byproducts of dysfunctional metabolic processes during photosynthesis when free chlorophyll molecules are illuminated (Supplementary Fig. S1).

Increasing evidence shows that chloroplast-generated ROS play a major role in the establishment of the HR [29,34]. It is proposed that SA, glutathione and Cys-Gly redox signaling contributes to both local defence and systemic acclimation response [39]. Moreover, the involvement of ROS in TMV induced lesion formation has been demonstrated and ROS also play an important role in the elevated production of ethylene and ethane compounds in damaged leaves [38]. Recent studies on the stress signaling molecules including SA, jasmonate (JA) in plant resistance to pathogens have been analysed to a large extent, and redox-based signaling appears to be more complex. It has been reported that FB1-induced plant PCD requires vacuolar processing enzyme (VPE) and phytohormones including salicylic acid (SA), jasmonate (JA) and ethylene (ET), while Bax Inhibitor-1 (BI-1) and extracellular ATP functions as an attenuator during this process [16–18,40]. However, direct evidence showing the molecular link between ROS and SA signaling in plant resistance to pathogens, especially in light-dependent PCD, has not yet been provided. In this work, we speculate that ROS, as an early consequence of biotic stress, play a positive role in regulation of SA signaling in FB1-induced cell death. Experimental results showed that pretreatment with ROS manipulators (CAT, AsA and DCMU) in Arabidopsis leaves significantly reduced FB1-induced SA content (Fig. 4E), suggesting that the synthesis of SA could be induced by ROS production. The fact that ROS-dependent cell death is associated with increased levels of SA in response to elicitors in our research providing a novel insight into crosstalk between ROS and phytohormones signaling molecules.

It has been reported that PAL induced by a variety of pathogens or pathogen-derived elicitors is necessary for SA synthesis [16,41], and PAL activity may be regulated by ROS accumulation [42]. In the present study, following pretreatment with the ROS manipulators, FB1-induced activation of PAL was dramatically suppressed (Fig. 4A, C), while PAL activity was shown an increasing tendency after exogenous H_2O_2 or 3-AT treatment (Fig. 4B, D). Exogenous H_2O_2 or 3-AT treatment further confirmed that ROS production can increase SA content in plant leaves (Fig. 4F). Together, our data demonstrate that FB1 can induce light-dependent ROS production at an early time point and then trigger PAL activation, which could initiate and regulate SA-mediated PCD. 3-AT has been widely used as a histidine synthesis inhibitor in yeast [43], while it acted as a reversible inhibitor of CAT in animal and plant cells, thus intracellular ROS accumulation can be achieved in our experiments by using this inhibitor [25,44,45]. Furthermore, we found that in contrast with the increase of PAL activity and *PAL1* gene expression, SA accumulation in H_2O_2-treated leaves was higher than 3-AT treatment within 1–4 days (Fig. 4F). The main cause for this is largely due to the versatile roles of H_2O_2 in plant cells. Experimentally, exogenous application of ROS or 3-AT treatment cannot duplicate the subtle aspects of HR-like cell death such as temporal and spatial localization. As revealed in a previous study, H_2O_2 can also induce the accumulation of free benzoic acid (BA) and salicylic acid (SA) in plant, and 2-hydroxylase that can be activated by H_2O_2 treatment is involved in catalyzing the formation of SA from BA [46,47]. Since FB1-induced the increase SA level was almost blocked by AIP in our experiment, it can be argued that ROS-mediated PAL activation plays a key role in the synthesis of SA (Fig. 5E, F).

In conclusion, our results suggest that light-dependent production of ROS including H_2O_2 and $O_2^{\cdot-}$ play a double-edged role in FB1-induced cell death process (Fig. 6). On the one hand, ROS can oxidize cell components and thus lead to, for example, degradation of chloroplast proteins. On the other hand, they can serve as second messengers and up-regulate SA synthesis by enhancing PAL activity in FB1-elicited HR-like cell death, which providing a new insight into the mechanisms of elicitor-triggered light-dependent cell death.

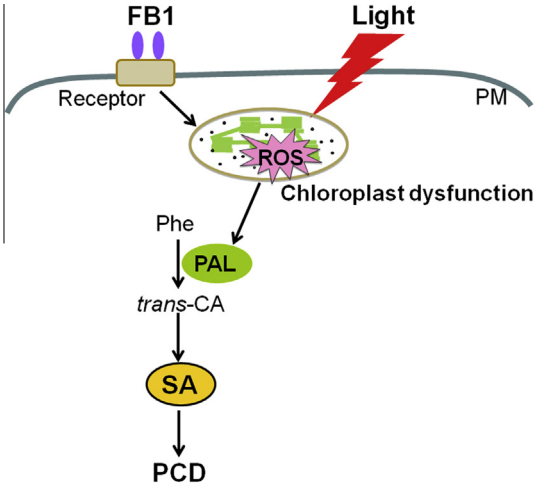

Fig. 6. A proposed chloroplast pathway model for ROS-mediated SA signaling pathways in plant-FB1 interactions. FB1, fumonisin B1; PAL, phenylalanine ammonia lyase; PM, plasma membrane; *trans*-CA, *trans*-cinnamate.

Acknowledgements

This research is supported by the Program for Changjiang Scholars and Innovative Research Team in University (IRT0829), the Key Program of NSFC-Guangdong Joint Funds of China (U0931005) and the National High Technology Research and Development Program of China (863 Program) (2007AA10Z204). We thank Professor Jerry Zon (Technical University in Wroclaw, Poland) for kindly providing AIP chemical, Professor Maureen R. Hanson (Cornell University, American) for kindly providing the transgenic Arabidopsis expressing stroma-targeted GFP, Dr. Caiji Gao (The Chinese University of Hong Kong, China) for critical reading of the manuscript.

Appendix A. Supplementary data

Supplementary data associated with this article can be found, in the online version, at http://dx.doi.org/10.1016/j.febslet.2013.05.034.

References

[1] Cvetkovska, M. and Vanlerberghe, G. (2012) Coordination of a mitochondrial superoxide burst during the hypersensitive response to bacterial pathogen in *Nicotiana tabacum*. Plant, Cell Environ. 35, 1121.
[2] Raffaele, S., Rivas, S. and Roby, D. (2006) An essential role for salicylic acid in AtMYB30-mediated control of the hypersensitive cell death program in Arabidopsis. FEBS Lett. 580, 3498–3504.
[3] Griebel, T. and Zeier, J. (2008) Light regulation and daytime dependency of inducible plant defenses in Arabidopsis: phytochrome signaling controls systemic acquired resistance rather than local defense. Plant Physiol. 147, 790–801.
[4] Montillet, J.-L. et al. (2005) Fatty acid hydroperoxides and H_2O_2 in the execution of hypersensitive cell death in tobacco leaves. Plant Physiol. 138, 1516–1526.
[5] Chernyak, B.V. et al. (2006) Production of reactive oxygen species in mitochondria of HeLa cells under oxidative stress. Biophysica Acta (BBA)-Bioenergetics 1757, 525–534.
[6] Díaz-Moreno, I., García-Heredia, J.M., Díaz-Quintana, A. and De la Rosa, M.A. (2011) Cytochrome *c* signalosome in mitochondria. Eur. Biophys. J. 40, 1301–1315.
[7] Yoshinaga, K., Arimura, S.-I., Niwa, Y., Tsutsumi, N., Uchimiya, H. and Kawai-Yamada, M. (2005) Mitochondrial behaviour in the early stages of ROS stress leading to cell death in *Arabidopsis thaliana*. Ann. Bot. 96, 337–342.
[8] Karpinski, S., Gabrys, H., Mateo, A., Karpinska, B. and Mullineaux, P.M. (2003) Light perception in plant disease defence signalling. Curr. Opin. Plant Biol. 6, 390–396.
[9] Gao, C., Xing, D., Li, L. and Zhang, L. (2008) Implication of reactive oxygen species and mitochondrial dysfunction in the early stages of plant programmed cell death induced by ultraviolet-C overexposure. Planta 227, 755–767.

[10] Li, Z., Xing, F. and Xing, D. (2012) Characterization of target site of aluminum phytotoxicity in photosynthetic electron transport by fluorescence techniques in tobacco leaves. Plant Cell Physiol. 53, 1295–1309.
[11] Liu, Y., Ren, D., Pike, S., Pallardy, S., Gassmann, W. and Zhang, S. (2007) Chloroplast-generated reactive oxygen species are involved in hypersensitive response-like cell death mediated by a mitogen-activated protein kinase cascade. Plant J. 51, 941–954.
[12] Zhang, L.R. and Xing, D. (2008) Methyl jasmonate induced production of reactive oxygen species and alterations in mitochondrial dynamics that precede photosynthetic dysfunction and subsequent cell death. Plant Cell Physiol. 49, 1092–1111.
[13] Li, Z. and Xing, D. (2011) Mechanistic study of mitochondria-dependent programmed cell death induced by aluminium phytotoxicity using fluorescence techniques. J. Exp. Bot. 62, 331–343.
[14] Wen, F., Xing, D. and Zhang, L. (2008) Hydrogen peroxide is involved in high blue light-induced chloroplast avoidance movements in Arabidopsis. J. Exp. Bot. 59, 2891–2901.
[15] Li, Z., Yue, H. and Xing, D. (2012) MAP kinase 6-mediated activation of vacuolar processing enzyme modulates heat shock-induced programmed cell death in Arabidopsis. New Phytol. 195 (1), 85–96.
[16] Asai, T., Stone, J.M., Heard, J.E., Kovtun, Y., Yorgey, P., Sheen, J. and Ausubel, F.M. (2000) Fumonisin B1-induced cell death in Arabidopsis protoplasts requires jasmonate-, ethylene-, and salicylate-dependent signaling pathways. Plant Cell 12 (10), 1823–1835.
[17] Stone, J.M., Heard, J.E., Asai, T. and Ausubel, F.M. (2000) Simulation of fungal-mediated cell death by fumonisin B1 and selection of fumonisin B1-resistant (fbr) Arabidopsis mutants. Plant Cell 12 (10), 1811–1822.
[18] Watanabe, N. and Lam, E. (2006) Arabidopsis Bax inhibitor-1 functions as an attenuator of biotic and abiotic types of cell death. Plant J. 45, 884–894.
[19] Zeier, J., Pink, B., Mueller, M.J. and Berger, S. (2004) Light conditions influence specific defence responses in incompatible plant-pathogen interactions: uncoupling systemic resistance from salicylic acid and PR-1 accumulation. Planta 219, 673–683.
[20] Turner, J.G. and Novacky, A. (1974) The quantitative relation between plant and bacterial cells involved in the hypersensitive reaction. Phytopathology 64, 885–890.
[21] Arnon, D.I. (1949) Copper enzymes in isolated chloroplasts. polyphenoloxidase in *Beta vulgaris*. Plant Physiol. 24, 1–15.
[22] Yin, R. et al. (2012) Feedback inhibition of the general phenylpropanoid and flavonol biosynthetic pathways upon a compromised flavonol-3-O-glycosylation. J. Exp. Bot. 63, 2465–2478.
[23] Herrera Medina, M.a.J., Gagnon, H., Piché, Y., Ocampo, J.A., Garcıa Garrido, J.M. and Vierheilig, H. (2003) Root colonization by arbuscular mycorrhizal fungi is affected by the salicylic acid content of the plant. Plant Sci. 164, 993–998.
[24] Guaragnella, N., Passarella, S., Marra, E. and Giannattasio, S. (2010) Knock-out of metacaspase and/or cytochrome *c* results in the activation of a ROS-independent acetic acid-induced programmed cell death pathway in yeast. FEBS Lett. 584, 3655–3660.
[25] Ferguson, I. and Dunning, S. (1986) Effect of 3-amino-1,2,4-triazole, a catalase inhibitor, on peroxide content of suspension-cultured pear fruit cells. Plant Sci. 43, 7–11.
[26] Zoń, J. et al. (2004) Experimental and ab initio calculated structures of 2-aminoindane-2-phosphonic acid, a potent inhibitor of phenylalanine ammonia-lyase, and theoretical studies of its binding to the model enzyme structure. New J. Chem. 28, 1048–1055.
[27] Sagi, M. and Fluhr, R. (2006) Production of reactive oxygen species by plant NADPH oxidases. Plant Physiol. 141, 336–340.
[28] Almagro, L., Ros, L.G., Belchi-Navarro, S., Bru, R., Barceló, A.R. and Pedreno, M. (2009) Class III peroxidases in plant defence reactions. J. Exp. Bot. 60, 377–390.
[29] Zurbriggen, M.D., Carrillo, N. and Hajirezaei, M.-R. (2010) ROS signaling in the hypersensitive response: when, where and what for? Plant Signal. Behav. 5, 393–396.
[30] Pastore, D., Laus, M.N., Di Fonzo, N. and Passarella, S. (2002) Reactive oxygen species inhibit the succinate oxidation-supported generation of membrane potential in wheat mitochondria. FEBS Lett. 516, 15–19.
[31] Amirsadeghi, S., Robson, C.A. and Vanlerberghe, G.C. (2006) The role of the mitochondrion in plant responses to biotic stress. Physiol. Plant. 129, 253–266.
[32] Popov, V., Simonian, R., Skulachev, V. and Starkov, A. (1997) Inhibition of the alternative oxidase stimulates H_2O_2 production in plant mitochondria. FEBS Lett. 415, 87–90.
[33] Nomura, H. et al. (2012) Chloroplast-mediated activation of plant immune signalling in Arabidopsis. Nat. Commun. 3, 926.
[34] Zurbriggen, M.D., Carrillo, N., Tognetti, V.B., Melzer, M., Peisker, M., Hause, B. and Hajirezaei, M.R. (2009) Chloroplast-generated reactive oxygen species play a major role in localized cell death during the non-host interaction between tobacco and *Xanthomonas campestris* pv. *vesicatoria*. Plant J. 60, 962–973.
[35] Mühlenbock, P. et al. (2008) Chloroplast signaling and lesion simulating disease1 regulate crosstalk between light acclimation and immunity in Arabidopsis. Plant Cell 20, 2339–2356.
[36] Hanson, M.R. and Sattarzadeh, A. (2011) Stromules: recent insights into a long neglected feature of plastid morphology and function. Plant Physiol. 155, 1486–1492.
[37] Izumi, M., Wada, S., Makino, A. and Ishida, H. (2010) The autophagic degradation of chloroplasts via Rubisco-containing bodies is specifically linked to leaf carbon status but not nitrogen status in Arabidopsis. Plant Physiol. 154, 1196–1209.
[38] Barna, B., Pogány, M., Koehl, J., Heiser, I. and Elstner, E. (2012) Induction of ethylene synthesis and lipid peroxidation in damaged or TMV-infected tobacco leaf tissues by light. Acta Physiol. Plant. 34, 1905–1914.
[39] Kuźniak, E., Kaźmierczak, A., Wielanek, M., Głowacki, R. and Kornas, A. (2012) Involvement of salicylic acid, glutathione and protein S-thiolation in plant cell death-mediated defence response of *Mesembryanthemum crystallinum* against *Botrytis cinerea*. Plant Physiol. Biochem. 63, 30–38.
[40] Chivasa, S., Ndimba, B.K., Simon, W.J., Lindsey, K. and Slabas, A.R. (2005) Extracellular ATP functions as an endogenous external metabolite regulating plant cell viability. Plant Cell 17 (11), 3019.
[41] Mauch-Mani, B. and Slusarenko, A.J. (1996) Production of salicylic acid precursors is a major function of phenylalanine ammonia-lyase in the resistance of Arabidopsis to *Peronospora parasitica*. Plant Cell 8 (2), 203–212.
[42] Xu, M. and Dong, J. (2005) O_2^- from elicitor-induced oxidative burst is necessary for triggering phenylalanine ammonia-lyase activation and catharanthine synthesis in *Catharanthus roseus* cell cultures. Enzyme Microbial Technol. 36, 280–284.
[43] Joung, J.K., Ramm, E.I. and Pabo, C.O. (2000) A bacterial two-hybrid selection system for studying protein–DNA and protein–protein interactions. Proc. Natl. Acad. Sci. 97, 7382–7387.
[44] Bagnyukova, T.V., Vasylkiv, O.Y., Storey, K.B. and Lushchak, V.I. (2005) Catalase inhibition by amino triazole induces oxidative stress in goldfish brain. Brain Res. 1052, 180–186.
[45] Amory, A., Ford, L., Pammenter, N. and Cresswell, C. (2006) The use of 3-amino-1,2,4-triazole to investigate the short-term effects of oxygen toxicity on carbon assimilation by *Pisum sativum* seedlings. Plant, Cell Environ. 15, 655–663.
[46] Lamb, C. and Dixon, R.A. (1997) The oxidative burst in plant disease resistance. Annu. Rev. Plant Biol. 48, 251–275.
[47] Leon, J., Lawton, M.A. and Raskin, I. (1995) Hydrogen peroxide stimulates salicylic acid biosynthesis in tobacco. Plant Physiol. 108 (4), 1673–1678.